One fairly definite example of the production of a charged V event in a p-p collision has been observed, and two doubtful cases of K-meson production. Therefore, the cross section for such events may well be comparable with that observed for π^--p at 1.37 Bev (similar energy available in the c.m. system), but the statistics are too poor to draw any definite conclusions concerning the production of heavy unstable particles.

Interpretation of Proton-Proton Interactions at Cosmotron Energies*

W. B. Fowler,[†] R. P. Shutt, A. M. Thorndike, and W. L. Whittemore,
Brookhaven National Laboratory, Upton, New York
V. T. Cocconi[‡] and E. Hart, *Cornell University, Ithaca, New York*
M. M. Block[§] and E. M. Harth, *Duke University, Durham, North Carolina*
E. C. Fowler, J. D. Garrison,[||] and T. W. Morris,[¶] *Yale University, New Haven, Connecticut*
(Received May 16, 1956)

In the absence of numerical predictions based on meson field theory, elastic p-p interactions have been compared with a simple optical model and inelastic ones with statistical theories and considerations based on charge independence. Elastic scattering data are fitted satisfactorily by a spherical interaction region with uniform density, radius 0.93×10^{-13} cm and absorption coefficient from 4.3 to 2.7×10^{13} cm^{-1}. Inelastic interactions provide a confirmatory test of charge independence at 0.81 Bev. Pion multiplicities at 1.5 and 2.75 Bev are higher than predicted by the Fermi statistical theory, but the difference is less than that observed for n-p interactions. The multiplicities observed for p-p interactions are lower than those calculated by Kovacs. Distributions of angle and momentum of particles, and correlation angle and Q values for pairs of particles, in general agree with the predictions of statistical theory at 0.81 Bev and disagree at 1.5 Bev. The data that are not consistent with statistical predictions suggest that a π-nucleon interaction may affect pion production in an important way, but the data are not sufficiently accurate for definite conclusions.

THE analysis of pictures of a H$_2$-filled diffusion cloud chamber exposed to proton beams from the Brookhaven Cosmotron has given the results reported in the preceding papers.[1] This paper gives a summary and tentative interpretations of the main features of the p-p collisions in the energy range from 0.8 to 2.75 Bev. These energies lie well above the threshold for meson production (0.29 Bev) and correspond to de Broglie wavelengths from 0.32 to 0.17×10^{-13} cm (in the c.m. system) which are considerably smaller than the range of nuclear forces. Consequently, the many reaction products listed in Table I of II and Table I of III are possible, and states of many different angular momenta may enter for each reaction.

A complete theory of mesons and nuclear forces would predict such phenomena from basic assumptions concerning the properties of meson and nucleon fields. In the absence of such a complete theory it is only possible to compare the data with greatly simplified models or with phenomenological considerations that apply to restricted portions of the data. One can, for example, assume that the nucleon-nucleon interaction through the pion field normally leads to production of π mesons in inelastic processes, and that the elastic scatterings are mainly a (diffraction scattering) consequence of the inelastic interactions. One can then obtain over-all information about the characteristics of the interaction region from analysis of the elastic events.

Such an assumption is a convenient one, since elastic and inelastic events then can be considered separately, as is done in the following discussion. The interrelation of elastic and inelastic events is probably more complicated, however, in actual fact.

A. ELASTIC AND INELASTIC CROSS SECTIONS

The procedure followed in estimating the total cross section for p-p collisions, σ_{tot}, from the cloud chamber data is described in I, Sec. C, II, Sec. B, and III, Sec. B, and the nature of the experimental uncertainties is discussed there. The results, in millibarns, are 45 ± 6, 35 ± 5, and 35 ± 5 for incident kinetic energies of 0.81, 1.5, and 2.75 Bev, respectively. It may be that these
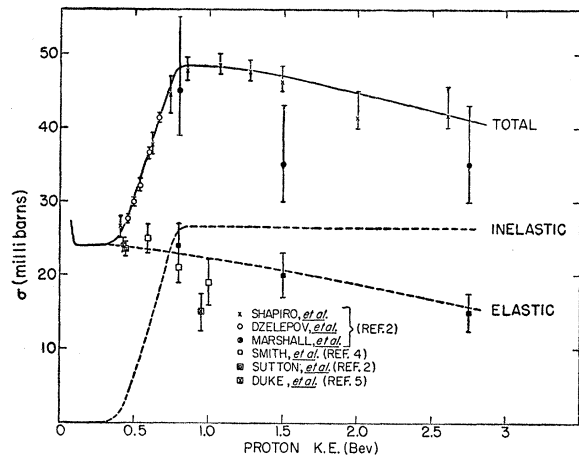
FIG. 1. Total elastic and inelastic p-p cross sections as functions of the kinetic energy of the incident proton. The curves drawn for σ_E and σ_I are tentative. Circles (O) and crosses (X) represent experimental points for σ_{tot} and squares represent points for σ_E. The solid symbols are the cloud chamber results where σ_E is computed from the σ_{tot} obtained with counters and the cloud chamber ratio for σ_E/σ_I. The other symbols show the results of other experiments.

figures should be increased somewhat because of systematic errors, but the correction is estimated to be $\leq 10\%$, and is neglected in the following discussion.

In Fig. 1, data from this and other experiments are summarized, showing σ_{tot} as a function of kinetic energy from 0.1 to 3.0 Bev. Several determinations of σ_{tot} from beam attenuation measurements with counters have been reported for energies below 1 Bev.[2] Counter results in the Bev region have been obtained recently by Chen, Leavitt, and Shapiro,[3] who have extended their measurements to 2.6 Bev. The cloud chamber results are in fair agreement with the counter data. Since the latter are determined with better statistical accuracy, the counter values for σ_{tot} will always be used in the following discussion. The interesting features of the curve for σ_{tot} are an approximately constant value of 24 mb from 0.10 to 0.40 Bev, followed by a sharp rise to a broad maximum of about 48 mb at about 1 Bev, and then by a slow decrease to a value of about 40 mb at 3 Bev.

As explained in I, Sec. D, II, Sec. C, and III, Sec. C, the detailed analysis of the cloud chamber scattering events has led us to the determination of the ratio between elastic and inelastic scatterings E/I, and hence to estimates of the partial elastic and inelastic cross sections, σ_E and σ_I, at each energy. The results are summarized in Table I. The values of σ_E given in column 4 are computed using our experimental ratios E/I and the counter values for σ_{tot} listed in column 3. Then $\sigma_I = \sigma_{tot} - \sigma_E$.

The cloud chamber results for σ_E are plotted in Fig. 1. Some other data on σ_E can be compared with these

[2] See references 4, 8, and 9 of I.
[3] Chen, Leavitt, and Shapiro, Phys. Rev. 103, 212 (1956).

results. Sutton et al. have estimated $\sigma_E = 23.8 \pm 1.2$ mb at 0.437 Bev from integration of their differential cross-section curve extrapolated toward small angles.[2] With a similar counter technique, Smith et al. have obtained values for σ_E of 24 ± 2, 25 ± 2, 21 ± 2, and 19 ± 3 mb at 0.44, 0.59, 0.80, and 1.00 Bev.[4] Recently Duke et al. have reported $\sigma_E = 15 \pm 2.5$ mb at 0.95 Bev from analysis of proton scattering in photographic emulsion.[5] The experimental evidence is too poor to warrant definite conclusions about the energy dependence of σ_E and σ_I. One may tentatively describe the elastic cross section as slowly decreasing with increasing energy from 0.4 to 3 Bev.[6] The sharp rise in total cross section above 0.4 Bev appears to be entirely due to inelastic interactions. The inelastic cross section is a few millibarns at 0.4 Bev, i.e., at about 0.1 Bev above the threshold for pion production. The inelastic cross section increases very rapidly up to approximately 0.8 Bev, and then probably levels off at a value around 26 mb. Inelastic events are already more numerous than elastic ones at 1 Bev and about twice as abundant at 3 Bev. Tentative curves for σ_E and σ_I are shown in Fig. 1.

Knowledge of σ_E and σ_I at even higher energies would obviously be of great interest. Experiments now in progress at Berkeley are expected to produce values for p-p cross sections at energies up to 6 Bev. Preliminary results obtained with a hydrogen-filled diffusion cloud chamber lead to a tentative value of σ_{tot} of 29.5 ± 5.5 mb at 5.3 Bev, based on 31 events, with inelastic scatterings more than five times as frequent as elastic scatterings.[7] From this result it would appear that σ_I is practically constant from 0.8 to 5 Bev, while σ_E decreases by 15 to 20 mb in the same energy range.

At even higher energies one has to depend on cosmic ray experiments for information about cross sections. The various cosmic-ray determinations of the proton reaction cross section on nuclei should in principle

TABLE I. Elastic and inelastic partial cross sections obtained from experimental data.

Proton energy (Bev)	Elastic to inelastic ratio, E/I	Total cross section, σ_{tot} (from counter results) (mb)	Elastic cross section, σ_E (mb)	Inelastic cross section, σ_I (mb)
0.81	1.04 ± 0.15	48	24 ± 2	24
1.5	0.74 ± 0.14	47	20 ± 2	27
2.75	0.59 ± 0.10	41	15 ± 2	26

[4] Smith, McReynolds, and Snow, Phys. Rev. 97, 1186 (1955).
[5] Lock, March, Muirhead, and Rosser, Proc. Roy. Soc. (London) A230, 215 (1955); W. O. Lock and P. V. March, Proc. Roy. Soc. (London) A230, 222 (1955); Duke, Lock, March, Gibson, McKeague, Hughes, and Muirhead, Phil. Mag. 46, 877 (1955).
[6] Cester, Hoang, and Kernan, Phys. Rev. 100, 940 (1955), and Phys. Rev. 103, 1443 (1956), this issue, have reported that the fraction of the total that is elastic at 3 Bev is as low as 20%, from emulsion observations. There may, however, have been some ambiguity in the identification of elastic scatterings on bound protons, due to their Fermi momentum.
[7] Wright, Saphir, Powell, Maenchen, and Fowler, Phys. Rev. 100, 1802(A) (1955).

supply some information in a wide energy range around 30 Bev. The energy spread of the protons is one source of uncertainty, and the results depend strongly on the geometry of the apparatus. In addition, deductions of the p-p reaction cross section have to rely either on difference methods (CH_2—C or D_2O—H_2O) that suffer from poor statistics and poor geometry, or on elaborate and somewhat arbitrary interpretations of the results obtained for heavy nuclei. The determinations based on difference methods furnish results for σ_I ranging from below 15 mb to approximately 80 mb.[8] The interpretation of the results for the heavy nuclei has led Williams to a higher value, $\sigma_I = 120_{-20}^{+30}$ mb.[9] One is, therefore, forced to conclude that the cosmic-ray data presently available do not provide reliable quantitative information.

B. ANGULAR DISTRIBUTION OF ELASTIC SCATTERING

The experimental definition of elastic scattering groups together all those events whose product is a proton with the same c.m. energy in the c.m. system as the incident one. It may, therefore, consist of both coherent and incoherent scattering, the latter arising from the possibility of spin-flip scattering whose amplitude cannot interfere with that of the nonflip amplitude. Therefore, $\sigma_E = \sigma_{\text{tot}} - \sigma_I = \sigma_{E,\text{coherent}} + \sigma_{E,\text{incoherent}}$. The total "reaction" cross section[10] is then given by $\sigma_{\text{reaction}} = \sigma_I + \sigma_{E,\text{incoherent}}$. The coherent scattering may be thought of as arising either from a nucleon-nucleon potential or from the absorption of the incident wave by inelastic processes, or both. Such scattered waves interfere, and the identity of the two contributions is lost in the interference. If waves of several angular momenta are involved, the interference leads to an angular distribution resembling an optical diffraction pattern, and therefore, such scattering is often termed diffraction scattering. From the observed angular distribution one can obtain information concerning the angular momentum states involved in the interaction, but there is no unambiguous way of determining to what extent incoherent scattering, potential scattering, or other coherent scattering is involved.

The experimental values of the elastic differential cross section, $d\sigma_E/d\Omega$, given in I, Sec. E, II, Sec. C, and III, Sec. C, are summarized in Fig. 2. The histograms give the differential cross section vs $\cos\theta^*$ (where θ^* is the scattering angle in the c.m. system) for 0.81, 1.5, and 2.75 Bev. The cloud chamber data at 0.81 Bev agree within the errors with the counter results of Smith et al. at the same energy.[4] Preliminary data of

[8] Walker, Dulles, and Sorrels, Phys. Rev. **86**, 865 (1952); Froman, Kenny, and Regener, Phys. Rev. **91**, 707 (1953); R. H. Rediker, Phys. Rev. **95**, 526 (1954); Cervasi, Fidecaro, and Mezzetti, Nuovo cimento **1**, 300 (1955); Watase, Suga, Tanaka, and Mitani, Nuovo cimento **2**, 1183 (1955).

[9] R. W. Williams, Phys. Rev. **98**, 1393 (1955).

[10] See, for example, J. M. Blatt and V. F. Weisskopf, Theoretical Nuclear Physics (John Wiley and Sons, Inc., New York, 1952), Chap. 8.
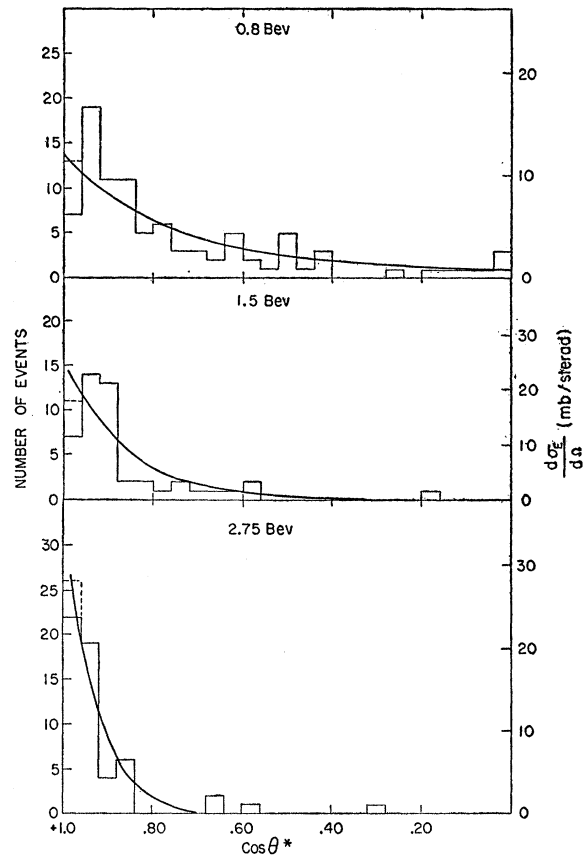
FIG. 2. Elastic differential cross sections at 0.81, 1.5, and 2.75 Bev. The histograms represent the experimental data corresponding to events with $\phi \geq 30°$; the broken line indicates the zenithal correction (see text). The curves are the angular distributions calculated using the optical model, with the assumptions listed in the text. The parameters used in the calculation are: $K = 4.3 \times 10^{13}$ cm^{-1}, $\sigma_E = 21.5$ mb (0.81 Bev); 3.7×10^{13} cm^{-1}, 21.0 mb (1.5 Bev); 2.7×10^{13} cm^{-1}, 16.0 mb (2.75 Bev). A value of $R = 0.93 \times 10^{-13}$ cm was used at all energies.

Cork and Wenzel at energies from 0.92 to 4.4 Bev are also consistent with our data.[11]

For the sake of comparison we have sketched the differential cross sections for proton energies of 0.345 and 0.59 Bev[2] along with our results in Fig. 3. The curve drawn for 0.345 Bev describes the behavior of the differential cross section from about 0.10 to 0.40 Bev; in this range, in fact, the striking features of $d\sigma_E/d\Omega$ are its isotropy and its approximate energy independence. As the incoming energy increases beyond 0.40 Bev, the behavior of $d\sigma_E/d\Omega$ changes drastically. The 90° value progressively decreases, and a peak at small angles develops. The forward peak is the only feature left at energies above 0.8 Bev, and its slope keeps increasing with energy, so that around 3 Bev practically no elastic scatterings occur at angles greater than 30° in the c.m. system. The onset of the forward peak coincides with the onset of the inelastic phenomena.

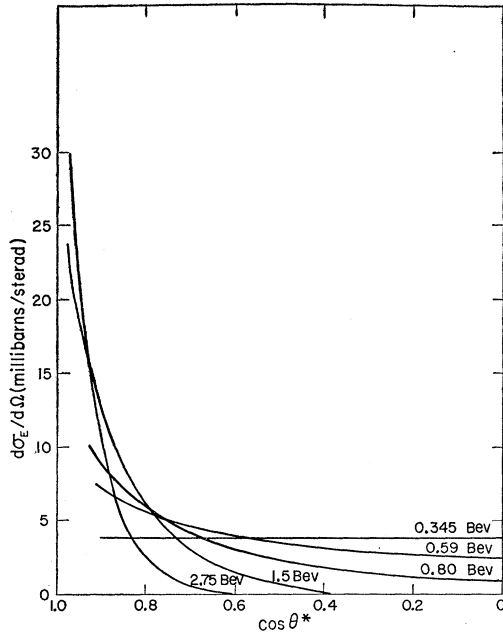[11] B. Cork and W. Wenzel, Phys. Rev. **100**, 962 (1955).

FIG. 3. Elastic differential cross sections for incident proton energies from 0.345 to 2.75 Bev. The curves for 0.345 and 0.59 Bev are derived from the experiments quoted in reference 2; the others are based on the cloud chamber results.

C. INTERPRETATION IN TERMS OF OPTICAL MODEL

For lack of any rigorous theory, it has become customary to use the formalism of the optical model developed for the interpretation of the interaction of neutrons with heavy nuclei[12] to analyze the results of high-energy elementary processes, like nucleon-nucleon collisions. The quantitative results obtained from such a crude model of a nucleon must be taken with some caution. One may hope, however, that the qualitative features of the phenomena are correctly described. Unfortunately, there are sufficient parameters available in the optical model (and the experimental data are uncertain enough) to allow one to put forward a number of versions all capable of fitting the experimental results, since one can choose both real and imaginary parts of the refractive index of nucleonic matter as well as the geometrical description of its density distribution.

The simplest set of assumptions compatible with the experimental results obtained for cross sections and angular distributions is the following:

(a) The interaction region is a sphere of uniform density.

(b) The radius, R, of the sphere is a constant, independent of energy.

(c) The sphere is purely absorbing. This is equivalent to saying that its refractive index has real part equal to unity (no potential scattering), and, therefore, the

[12] Fernbach, Serber, and Taylor, Phys. Rev. **75**, 1352 (1949).

incoming wave undergoes amplitude attenuation in it but no modification of its wavelength.

(d) Incoherent elastic scattering is negligible.

With these assumptions, the set of parameters compatible with the experimental results is as given in Table II. The compatible values for R, σ_E and σ_I are deduced from the Bethe-Wilson curve for $k_1\lambda=0$.[13] The absorption coefficient, $K=1/\lambda$, is deduced from Fernbach, Serber, and Taylor, Eq. (5). The opacity is the ratio $\sigma_I/\pi R^2$. Under these assumptions, the opacity decreases slowly as the energy of the incoming proton increases, and hence the absorption coefficient does the same. The opacity is close to unity, but a totally black interaction region could not describe the results at all energies, as it would produce equal elastic and inelastic cross sections, which would certainly be inconsistent with the experimental results.

The differential cross section was calculated with the values for R and K listed in Table II, using Eq. (7) of Fernbach, Serber, and Taylor. The results are shown by the curves drawn in Fig. 2. They can be considered in fair agreement with the experiments.

None of the assumptions listed above has any real justification except simplicity. It seems likely that density distributions with no sharp edges (Gaussian or tapered distributions) should be better representations of a nucleon than a uniform sphere. One might, of course, prefer discontinuous distributions with an opaque or semi-opaque core, surrounded by a region of weaker interaction, analogous to the Jastrow or Lévy potentials.[14] The data are not, however, sufficiently detailed to distinguish between the many possibilities.[15] It may well be that the size of the interaction region varies with the energy of the incoming particle, in which case the assumption of a constant radius for the interaction region just happens to be usable in this particular energy range. The variation of R with energy would probably be slow, however. The preliminary Berkeley results at 5.3 Bev could also be fitted with a radius of about 1.0×10^{-13} cm. One would have to

TABLE II. Optical-model parameters fitting experimental results.

Proton energy (Bev)	Radius, R (cm)	Absorption coefficient, K (cm^{-1})	Opacity	Calculated elastic cross section σ_E (mb)	Calculated inelastic cross section σ_I (mb)
0.81	0.93×10^{-13}	4.3×10^{13}	0.97	21.5	26.5
1.5	0.93×10^{-13}	3.7×10^{13}	0.96	21.0	26.0
2.75	0.93×10^{-13}	2.7×10^{13}	0.92	16.0	25.0

[13] H. A. Bethe and R. R. Wilson, Phys. Rev. **83**, 690 (1951).
[14] R. Jastrow, Phys. Rev. **81**, 165 (1951); M. M. Lévy, Phys. Rev. **88**, 725 (1952).
[15] Calculations with a Gaussian distribution showed that the index of refraction would then have to include an appreciable real part because the contribution of the weakly interaction periphery would otherwise give too much reaction cross section relative to the elastic. This would probably be true of any distribution with a fuzzy edge.

assume, however, that the opacity of the interaction region is reduced to about 0.6 at that energy. Assumptions (c) and (d) may prove wrong, particularly at 0.81 Bev. In fact, at energies below threshold for pion production there is no inelastic scattering, and at energies not far above threshold inelastic scattering is rare, so that the index of refraction of nucleonic matter is predominantly real. The onset of inelastic phenomena is expected to cause a change from predominantly real to predominantly imaginary index of refraction. At 0.81 Bev the change may well not be complete, and potential scattering may still given an appreciable contribution to the coherent components of the outgoing wave. In addition, incoherent elastic components arising from spin-flip scattering may be of importance. No satisfactory way was found to evaluate the different contributions to elastic scattering at these energies theoretically. However, as said before, the simplifying assumptions used find justification in the fact that our experimental data do not require the introduction of more parameters.

Fortunately, the main conclusion that can be derived from the results on elastic scattering at Cosmotron energies is independent of detailed interpretations. The conclusion is that in p-p collisions the interaction region acts like an almost opaque absorbing body with dimensions of the order of 1.0×10^{-13} cm. One may speculate on the relation of this observation to the results obtained in interpreting p-p elastic scattering in the energy region between 0.15 and 0.40 Bev. In fact, the theories proposed have as a common feature the postulate of a region of repulsion, i.e., a "hard or reflecting core," strong enough to overcompensate the attractive interactions, with dimensions between 0.5 and 1.0×10^{-13} cm. The Cosmotron results may indicate that as the energy increases the hard core begins to be "penetrated" and can be considered as an almost opaque body of similar dimensions.

The optical-model formalism was also applied to π^--p scattering at 1.4 Bev, and led to conclusions similar to those for p-p scattering. The elastic scattering could be described as caused by a sphere with $R=1.2 \times 10^{-13}$ cm and opacity 0.6.[16] The numerical values for the radii and opacities may not have enough significance to warrant comparisons and speculations on their relative values. However, the fact that the two experiments yield similar results should be noted. The relation between the two results should be predicted by any complete theory of meson and nucleon fields. In the absence of such a theory, we can only offer two qualitative comments:

(a) If one wants to interpret the radius of the interaction region in π-p collisions as the distance to which the interacting material of a nucleon (presumably its meson cloud) extends, one might think that nucleon-nucleon interaction can occur as soon as the

interacting material of the two nucleons overlaps. Following this idea, the radius of the p-p interaction region should be greater than that for π-p, while it actually appears to be slightly smaller.

(b) If, on the other hand, the π-p interaction is considered as "the fundamental interaction," one might think that the apparent radius of the π-p interaction region may be larger than the radius for p-p collisions.

Further speculations on this subject seem premature at present.

D. PION MULTIPLICITY IN INELASTIC EVENTS

In discussing inelastic events, the first step is to consider the over-all frequency of different pion multiplicities before going to a more detailed breakdown in terms of final charge states and distributions in energy and angle of the particles emitted. Since many different reactions are possible, the analysis of inelastic events is much more complicated than that of elastic events. No detailed theory is available for comparison, but various aspects of the data can be compared with the Fermi statistical theory, which makes no specific assumptions concerning the interaction of pion and nucleon fields.[17] If the experimental results show departures from the predictions of the statistical theory, these may give information concerning the details of the interactions involved. One detail which may be of particular interest is the strong interaction in the pion-nucleon state with $T=J=3/2$ shown by pion-nucleon scattering results.[18] It is, therefore, important to determine whether pion production phenomena are influenced by such a strongly-interacting state.

In I, II, and III, results were obtained for the frequency of single, double, and triple pion production. The "best values" are summarized in Table III, where they are compared with theoretical predictions. The third column gives the results of an evaluation of the Fermi theory using exact relativistic expressions.[19] The

TABLE III. Comparison of experimental multiplicities with theory.

Proton energy (Bev)	Experimental ratios single:double:triple	Theoretical ratios	
		Fermi single:double:triple	Kovacs single:double
0.81	100: 0: 0	100: 0:0	100: 0
1.5	80:20: 0	94: 6:0	55:45
2.75	36:48:16	78:20:2	28:72[a]

[a] Extrapolated linearly from Kovacs' curves.

[16] Eisberg, Fowler, Lea, Shepard, Shutt, Thorndike, and Whittemore, Phys. Rev. 97, 797 (1955).

[17] E. Fermi, Progr. Theoret. Phys. Japan 5, 570 (1950); or E. Fermi, Phys. Rev. 92, 452 (1953); 93, 1435 (1954).
[18] See, for example, H. A. Bethe and F. de Hoffmann, Mesons and Fields (Row, Peterson and Company, Evanston, 1955), Vol. 2, or Proceedings of the Rochester Conference on High-Energy Nuclear Physics, 1955 (Interscience Publishers, Inc., New York, 1955).
[19] M. M. Block, Phys. Rev. 101, 796 (1956). In the Fermi theory the radius of the interaction volume in which equilibrium is supposed to take place is an unspecified parameter that can in principle be adjusted to fit experiment. The calculations quoted

experimental results at 1.5 and 2.75 Bev show considerably more double and triple meson production than predicted. This conclusion is similar to that obtained from analysis of n-p collisions.[20]

A number of theoretical calculations have been made in which the Fermi theory is modified in different ways. Lepore and Neuman introduced the conservation law of relativistic center-of-energy.[21] Qualitatively, their results predict a lowering of the average momentum of the pion (in comparison with the original Fermi theory), resulting in a higher multiplicity. Since no detailed calculations have been made at our specific energies, however, it is not known whether this theory gives quantitative agreement with our results. Bocchieri and Feldman have calculated matrix elements by a perturbation calculation and have shown that a sufficiently large coupling constant might lead to frequent double pion production.[22] The effects of final state interactions between nucleons and between pions and nucleons have been included by Kovacs.[23] He finds that the pion-nucleon interaction seriously alters the statistical results, with an enhancement of two-meson states due to resonance effects. If this effect dominates the production process, one would expect the cross section for single meson production to rise sharply at a laboratory kinetic energy of $\sim$0.7 Bev, whereas double meson production should compete seriously at $\sim$1.5 Bev, and triple production should set in at $\sim$2.4 Bev. This is in good qualitative agreement with our experimental results. Kovacs' calculated results for the single:double pion production ratios are indicated in column 4 of Table III. The theoretical multiplicities are somewhat larger than the experimental ones, but this discrepancy might well be ascribable to the approximate calculation methods employed, in particular, the nonrelativistic treatment of the nucleons.

Of course, the experimental results are not altogether free from uncertainties, as pointed out in I, II, and III. Rough confirmation of the high multiplicities can be obtained from the emulsion data of Cester, Hoang, and Kernan at 3 Bev whose single:double:triple ratios are 43:45:12.[6]

E. PARTIAL CROSS SECTIONS AND CHARGE INDEPENDENCE

For a given pion multiplicity we now investigate the relative frequencies of the various possible charge states. The concept of charge independence of nuclear forces has proved to be a valuable tool in the analysis of high-energy nuclear reactions and the following dis-

cussion is based on the charge-independence hypothesis. Two simplifying assumptions concerning charge states have been advanced by Fermi[17] and by Peaslee.[24] Fermi assumes that all accessible final states are equally probable, while Peaslee assumes that only final states resulting from an intermediate $T=3/2$ state are to be counted. The resulting statistical weights are summarized in Table IV. Despite the differences in assumption, the relative weights of different charge states are not widely different. When these predictions are compared with the experimental results in Table II of I, Table III of II, Table II of III, and Table III of III, one finds no obvious decision in favor of either Fermi or Peaslee weights.

It is, therefore, necessary to consider the question in more detail. Experimentally the most reliable data are those at the lowest energy, where measurements are most accurate and criteria of identification least ambiguous. Consequently, the $(pn+)$ to $(pp0)$ ratio, R, is of the most significance; the Fermi value for this ratio is 3:1, and Peaslee value is 5:1. The values of R obtained experimentally from identified $(pn+)$ and $(pp0)$ events are 87/5 at 0.81 Bev, 19/0 at 1.5 Bev, and 10/3 at 2.75 Bev, but the 2.75-Bev ratio is too unreliable to be of use. The 0.81-Bev data also include 16 events that could be either $(pn+)$ or $(pp0)$. Since it is exceedingly unlikely that a major fraction of the uncertain cases are $(pp0)$, it is concluded that $R=17\pm8$, where the limits include the effects of both statistical fluctuations and the uncertainty in the distribution of the unidentified events. At 1.5 Bev the number of unidentified events is relatively larger, but the value of R appears also to be high.

We therefore conclude that our value of R does not fit either the Fermi or the Peaslee prediction. The more general deductions from the charge-independence hypothesis, presented in the appendix, give results that

TABLE IV. Statistical weights for different final charge states from p-p interactions.

| Multiplicity | Charge state | Relative statistical weight[a] | | |
		Fermi	Peaslee	Kovacs
Single	$(pn+)$	3	5	1
Single	$(pp0)$	1	1	0
Double	$(pn+0)$	9	26	$\sim$12
Double	$(pp00)$	2	8	$\sim$ 6
Double	$(nn++)$	3	2	$\sim$ 9
Double	$(pp+-)$	6	9	$\sim$17
Triple	$(pn+00)$	121	68[b]	
Triple	$(pp000)$	18	8	
Triple	$(nn++0)$	72	14	
Triple	$(pp+-0)$	154	66	
Triple	$(pn++-)$	175	114	

[a] The figures give the relative statistical weight of different charge states for a given multiplicity, but they are not to be used for comparison between different multiplicities.

[b] These figures are based on a hypothetical intermediate state consisting of two $T=3/2$ (nucleon+pion) states with an additional unaffiliated pion.

were made with radius equal to the Compton wavelength of the pion, as is conventional. The results of Sec. C suggest that the actual region of interaction may be somewhat smaller. This would tend to reduce the predicted multiplicity, giving even poorer agreement with experiment.

[20] Fowler, Shutt, Thorndike and Whittemore, Phys. Rev. **95**, 1026 (1954).

[21] J. V. Lepore and M. Neuman, Phys. Rev. **98**, 1484 (1955).

[22] P. Bocchieri and G. Feldman, Phil. Mag. **45**, 1145 (1954).

[23] J. S. Kovacs, Phys. Rev. **101**, 397 (1956).

[24] D. C. Peaslee, Phys. Rev. **94**, 1085 (1954); **95**, 1580 (1954).

do not depend on any specific model for the $(pn+)$ and $(pp0)$ reactions, and permit an interpretation of the large value of R. The appendix shows that if r is defined as the ratio of differential cross sections

$$r=d\sigma(pn+)/d\sigma(pp0), \qquad (1)$$

then, in general,

$$r=1+2|\Phi_S|^2/|\Phi_A|^2, \qquad (2)$$

where Φ_S is that (real space)$\times$(real spin) portion of the outgoing wave function which is symmetric under nucleon exchange and Φ_A is the similar portion which is antisymmetric. In particular, $r=\infty$ occurs when the (real space)$\times$(real spin) wave function is symmetric, i.e., $\Phi_A=0$, which then gives $R=\infty$ for the over-all ratio (including all angles, momenta, etc). Further, it was shown that if $r=1$ or if $r=\infty$ (for all angles, momenta, etc.), then a consequence of charge independence is that the neutron and proton in the $(pn+)$ reaction have *identical* angular distributions, momentum distributions, etc.

The experimental data do not give $R=\infty$, but only $R=17\pm8$. Using this range of R values, it is found that between 80% and 95% of the cross section for single pion production is due to Φ_S. Therefore, the major effects in this experiment can be attributed to Φ_S, and it is approximately correct to neglect Φ_A in comparison. It therefore follows from the preceding arguments that charge independence requires that the proton and neutron have the same spatial distributions (if Φ_A is set equal to zero). As will be shown in later sections, we find experimentally that the proton and neutron do indeed have similar distributions, within experimental error. Thus this result provides a check on the hypothesis of charge independence of nuclear forces at 0.81 Bev, an energy considerably higher than those at which other checks have been made.[25] Similar conclusions would hold at 1.5 and 2.75 Bev, but the values of R are not as well determined.

The functions Φ_S and Φ_A are associated with the isotopic spin functions which are antisymmetrical and symmetrical, respectively. These isotopic spin functions are obtained from the addition of the isotopic spins of the two nucleons to form states of $T'=0$ and $T'=1$, with subsequent addition of the pion isotopic spin. An alternative model involves addition of the isotopic spins of pion and one nucleon to form $T'=3/2$ and $T'=1/2$ states, with subsequent addition of the other nucleon's isotopic spin. This may be considered as a more general form of the Peaslee model. It is also discussed in the appendix, and the result is obtained that values of R larger than 5 and smaller than 2 can only occur because of interference terms between 3/2 and 1/2 states. Because of the 1/2 state contributions and
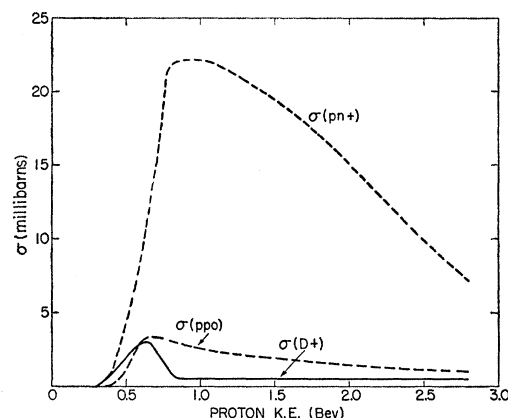

FIG. 4. Rough estimate of partial cross sections for $(d+)$, $(pn+)$, and $(pp0)$ reactions as a function of proton kinetic energy in laboratory system. Curves up to 0.7 Bev are based on references 2 and 11. Above 0.7 Bev the curves are a guess based on our rough experimental points.

the consequent large interference terms that are present for the large values of R found in this experiment, this excited nucleon model loses its simplicity and most of its predictive powers.

The energy dependence of the partial cross sections for single meson production is also of interest. There are three possible reactions, $(d+)$, $(pn+)$, and $(pp0)$. The data given in I, Sec. D, II, Sec. C, and III, Sec. C show that $(d+)$ is negligible and that $(pp0)$ is a small contribution at these energies. The number of ambiguous events at 1.5 and 2.75 Bev is too large to permit an accurate determination of the $(pp0)$ contribution at 1.5 and 2.75 Bev, but it appears that the energy dependence of $(d+)$, $(pn+)$, and $(pp0)$ reactions may have the qualitative features shown in Fig. 4. For double and triple meson production, the information on partial cross sections for different charge states is not complete enough to warrant drawing similar curves.

The $(d+)$ reaction is the most probable immediately above threshold, and reaches a maximum cross section of about 3 mb,[26] but above 0.8 Bev $(d+)$ events are very rare. Apparently the two nucleons are seldom left with low enough relative energy to emerge in the bound state.

The $(pp0)$ reaction is practically forbidden at threshold[27] but it is unlikely that the same selection rule accounts for its small cross section in the high-energy region. The $(pn+)$ reaction predominates for energies above about 0.4 Bev. The occurrence of a maximum for both $(pp0)$ and $(pn+)$ cross sections at approximately the same energy and the slow decrease of both beyond 0.8 Bev appear to be due to the onset of competition of multiple meson production.

[25] For a summary of experiments testing charge independence, see Henley, Ruderman, and Steinberger, *Annual Review of Nuclear Science* (Annual Reviews, Inc., Stanford, 1953), Vol. 3, p. 1.

[26] M. G. Meshcheryakov and B. S. Neganov, Doklady Akad. Nauk. S.S.S.R. **100**, 677 (1955).
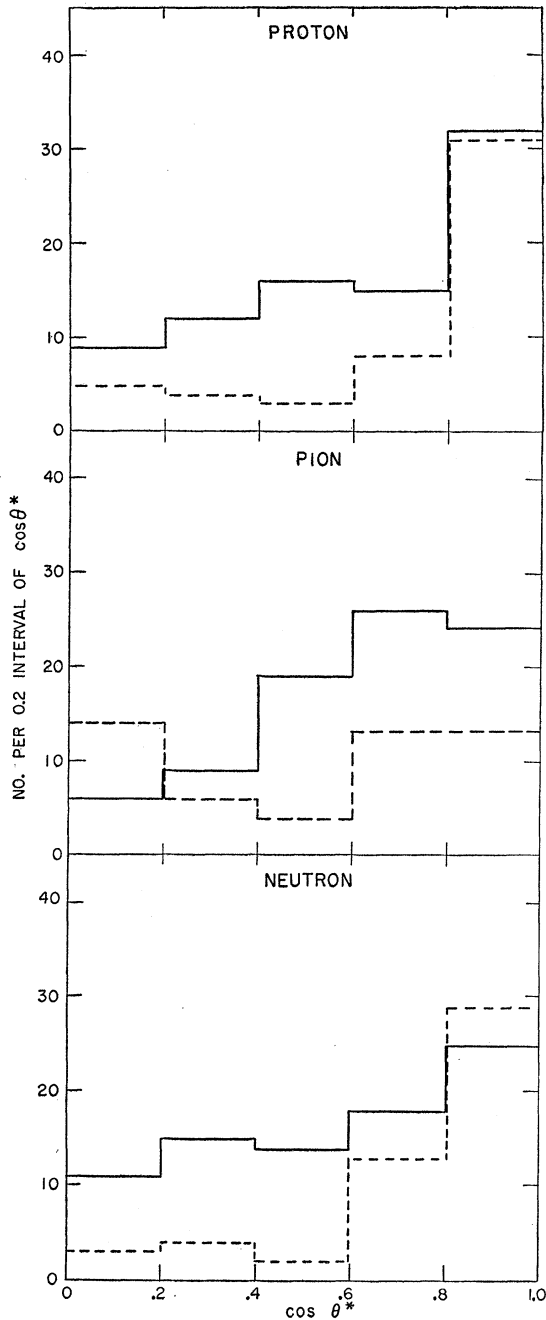[27] See, for example, A. H. Rosenfeld, Phys. Rev. **96**, 139 (1954).

FIG. 5. Angular distribution of protons, neutrons, and pions in (pn+) events at 0.81 Bev (solid lines) and 1.5 Bev (broken lines).

F. ANGULAR DISTRIBUTIONS FOR (pn+)

Since the (pn+) reaction is the most frequent, it is the only one having a sufficient number of cases for angle and momentum distributions to be meaningful. There are few definite theoretical predictions concerning angular distributions with which the experimental data can be compared. Of course all angular distributions in the c.m. system should show forward-backward sym-

metry about 90°, since the two colliding protons are identical particles. The simple statistical model (in which angular momentum is not conserved) would predict isotropy for all of the particles. Fermi has shown that at very high energies, where there is an appreciable Lorentz contraction of the sphere into which energy is deposited, the conservation of angular momentum requires a strong forward-backward peaking in the c.m. system.[17] It is not clear whether, at the rather low energies of these experiments, this effect would lead to appreciable anisotropy in the c.m. system. Near threshold it is usually assumed that the nucleons are emitted in S states and pions in P states, and one might expect the same states to predominate at higher energies, as was assumed by Kovacs.[23] In such a case the nucleons should be fairly isotropic, but the pions peaked forwards and backwards. The argument presented in IV, Sec. E leads to the conclusion that the symmetric function Φ_S predominates, and therefore, neutron and proton should have similar angular distributions, whatever the distribution is.

When the experimental distributions given in I, Sec. F, II, Sec. D, and III, Sec. E are tested for symmetry about 90°, we find appreciable asymmetries, which are greatest for 2.75 Bev and least for 0.81 Bev. As previously pointed out, these must be ascribed to bias arising largely from the fact that events with charged particles emitted backward in the c.m. system are easiest to identify. It is difficult to determine the extent to which this bias will modify other distributions. Since the bias is worst for 2.75 Bev and the data fewest, distributions at this energy will not be discussed. In order to reduce the bias at the lower energies, all distributions were folded about 90°. The resulting angular distributions are plotted in Fig. 5. The nucleon distributions show a marked forward-backward preference in all cases. They are certainly not consistent with S wave or other isotropic emission, but suggest a collision with low momentum transfer, that is quasi-elastic in character. At each energy proton and neutron distributions are similar and could be identical within the experimental errors, as predicted in Sec. E. On the other hand, the data certainly do not rule out the possibility of minor differences between neutron and proton distributions; such differences might arise from interference between Φ_S and Φ_A, even though Φ_A is relatively small.[28]

The pion angular distribution at 0.81 Bev does indeed resemble a P-wave angular distribution, having a minimum at 90°. The 1.5-Bev distribution, however, appears essentially isotropic.

In principle one should be able to obtain information on the values of the angular momentum of the system

---

[28] Another condition has to be fulfilled if the neutron and proton are to be interchangeable. It is the symmetry about the 0°–180° axis of the distribution of the function $(\phi_p - \phi_n)$ where ϕ_p is the azimuth angle of the proton relative to any arbitrary direction, and ϕ_n is the azimuth angle of the neutron. It is found that this condition is fulfilled within the accuracy of the experiment.

by an examination of the angular distributions. It was shown earlier that the major portion of the (real space) X (real spin) part of the total wave function is symmetric in the interchange of the nucleons. If analysis of the spatial distributions were to show that the real-space portion was of only one symmetry, e.g., symmetric, then we would be able to conclude that the two nucleons were interacting in a particular real spin state, e.g., the triplet state. In practice the analysis of the data from this point of view presents formidable difficulties and has not been attempted.

G. MOMENTUM DISTRIBUTIONS FOR $(pn+)$

The momentum distributions expected on the basis of the Fermi statistical theory have been calculated using exact relativistic expressions.[19] The curves given in Fig. 6 show the results for 0.81 Bev and 1.5 Bev. It should be emphasized that the shape of the momentum distribution for a given multiplicity does not depend on the interaction volume. The discussion of Sec. E indicates that proton and neutron should have approximately the same momentum and angular distributions. Other predictions can be made only qualitatively. In the work of Lepore and Neuman, the pion would be emitted with lower average momentum than that predicted by the Fermi theory. The calculations of Kovacs also give lower pion momenta than the Fermi theory for incident proton energies greater than about 1 Bev.

The experimental momentum distributions are the histograms plotted in Fig. 6. The results at 0.81 Bev fit well with Fermi theory curves for both proton, neutron, and π^+. Differences between proton and neutron, if any, are small. The experimental distributions at 1.5 Bev, however, are not consistent with the Fermi predictions. The statistical factor predicts a peak at too low a momentum for the nucleon distribution and at much too high a momentum for the pion. The results of Lepore and Neuman and Kovacs would give better agreement with experiment at 1.5 Bev. Proton and neutron spectra are again similar at 1.5 Bev, so that the predictions of Sec. E are confirmed.

If one compares pion distributions at 0.81 and 1.5 Bev, it is evident that the difference between them is much less than one predicts on the basis of Fermi theory. Yuan and Lindenbaum have noted that the pion energy spectrum in the c.m. system from nucleon-nucleon collisions does not change much with incident nucleon energy.[29] They have interpreted this in terms of a strong effect of the pion-nucleon resonance. Our momentum spectra are in rough agreement with their observation, but the $(pn+)/(pp0)$ ratio of 17 indicates that pion production does not occur entirely through a $T=J=3/2$ intermediate state, as shown in Sec. E.

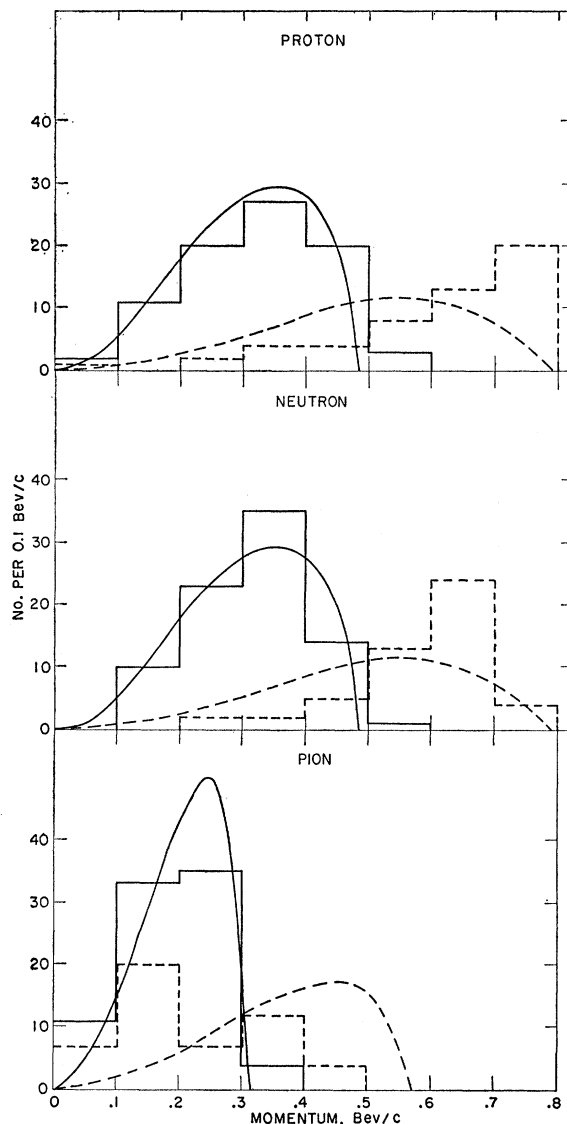[29] L. C. L. Yuan and S. J. Lindenbaum, Phys. Rev. **93**, 1431 (1954).

FIG. 6. Momentum distributions of protons, neutrons, and pions in $(pn+)$ events at 0.81 Bev (solid lines) and 1.5 Bev (broken lines). The histograms represent the experimental data and the smooth curves the distributions predicted by statistical theory.

H. Q VALUES BETWEEN PAIRS OF PARTICLES

Interactions between pairs of particles, such as a pion-nucleon interaction, might be expected to be shown most directly by an effect on the distribution of relative energy, or Q value, between pairs of particles.[30] For example, a resonant $T=3/2$ interaction would

[30] It should be pointed out that for collisions with three-body final states and unique energy in the c.m. system, such as $(pn+)$, the Q plots are not kinematically independent of the momentum distributions but rather are alternative means of analyzing the same data. In particular, a specification of the neutron momentum distribution automatically determines the Q_{p+} distribution. However, the Q plots do serve as independent approaches for collisions involving 4 or more final-state particles.
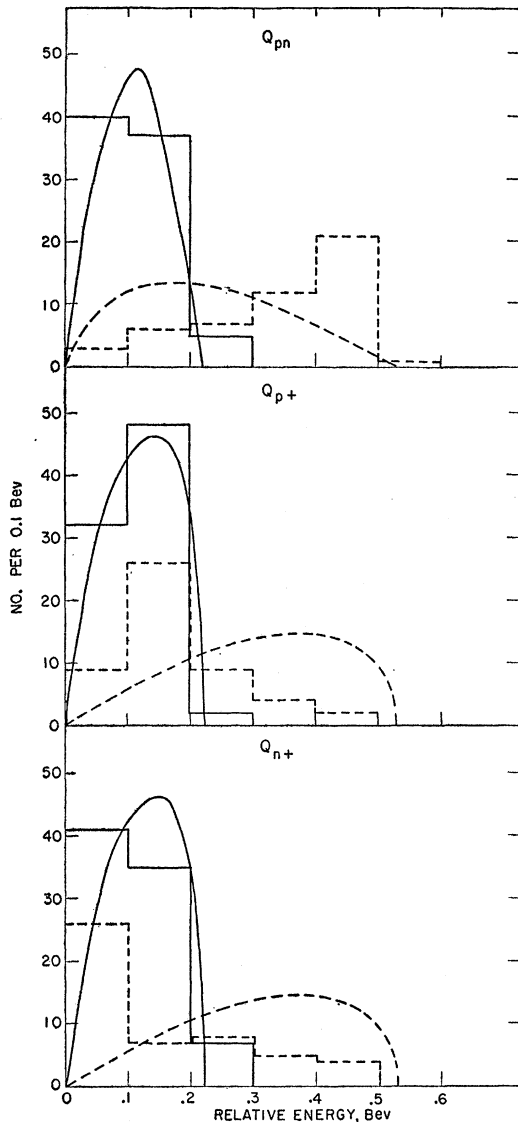
FIG. 7. Q-value distributions for (pn), $(p+)$, and $(n+)$ pairs of particles in $(pn+)$ events at 0.81 Bev (solid lines) and 1.5 Bev (broken lines). The histograms represent the experimental data and the smooth curves the distributions predicted by statistical theory.

strongly affect the Q_{p+} distribution. Calculations based on the Fermi theory have been made to predict Q-value distributions that would exist in the absence of important 2-particle interactions.[19]

Figure 7 shows Q-value distributions for $(p+)$, $(n+)$, and (pn) pairs from 0.81- and 1.5-Bev $(pn+)$ events as observed experimentally and as predicted from the Fermi theory. At 0.81 Bev reasonable agreement is obtained. Also, the agreement between Q_{p+} and Q_{n+} distributions supports our earlier conclusion that charge independence is satisfied. At 1.5 Bev the statistical predictions are in marked disagreement with the data. There appears to be a difference between Q_{p+} and Q_{n+}

distributions, but it is difficult to be sure whether this difference is significant because of the large number of uncertain classifications, statistical fluctuations, measurement errors, and possible biases. It certainly does not imply any failure of charge independence at 1.5 Bev.

As was noted in II, Sec. E, the average value of Q_{p+} is 154 Mev for the 1.5-Bev cases, which would agree well with the energy of the π^+-p scattering resonance. For the 0.81-Bev data, the average value of Q_{p+} is about the same, but similar values are predicted by the statistical calculations. Further measurements with greater accuracy are necessary to show whether the 1.5-Bev result is really caused by the π-p resonance or whether the numerical agreement is merely fortuitous.[31]

I. ANGULAR CORRELATIONS BETWEEN PAIRS OF PARTICLES

The distributions of angles (in the c.m. system) included between particle pairs from $(pn+)$ reactions are shown in Fig. 7 of I for 0.81 Bev, in Fig. 5 of II for 1.5 Bev, and in Fig. 6 of III for 2.75 Bev. A striking feature at all beam energies is the strong back-to-back correlation between proton and neutron. This, of course, mainly reflects the fact that the average nucleon momentum is considerably higher than that of the average pion; consequently, momentum conservation in the c.m. system requires that the nucleons be emitted almost antiparallel.

There appears to be a strong preference for large pion-proton correlation angles in $(pn+)$ events at 0.81 Bev, which is somewhat less pronounced for the pion-neutron pair. However, these apparent differences are probably too small to be conclusive. It should be noted that the kinematics of a 3-body final state are such that a specification of two correlation angles suffices to specify the magnitudes of all momenta. Thus, if the (π^+,p) and (π^-,n) angular correlation distributions are dissimilar, this would result in a dissimilarity between the proton and neutron *momentum* distributions. Since we had concluded that there were no obvious differences in the momentum spectra of the two nucleons, the small apparent asymmetry in angular correlations may be spurious. On the other hand, there may in fact be a small difference between neutron and proton momentum distributions.

The angular correlation data at 1.5 Bev for $(pn+)$ events show that the (π^+,p) pair has a small peak at large angles whereas the (π^+,n) pair peaks slightly at small angles. A similar difference was noted in the Q-value distributions, but the statistical accuracy of these results is low. Charge independence predicts that for a $(pn+)/(pp0)$ ratio of ∞, the proton and neutron would have the same behavior. It is possible that the

---

[31] One might hope to obtain further information from the 2.75-Bev data, but since there are only 10 $(pn+)$ events and 17 $(pn+0)$ ones, with severe problems concerning bias and identification, no clear conclusions can be reached.

asymmetry in these observations is due to experimental errors. It is also possible that a small but nonvanishing Φ_A would give rise to small asymmetries by interference with the dominant Φ_S.

J. CONCLUSIONS

The rise in total cross section for p-p interactions occurring between 0.4 and 0.8 Bev is due to inelastic events leading to the production of one or more pions, the cross section for such processes being about 26 millibarns for energies from 0.8 to 2.75 Bev. In this energy range, the elastic cross section apparently drops slowly with increasing energy.

The ratio of elastic to inelastic cross sections and the strong forward peaking of the elastic cross section are consistent with predictions of a simple optical model in which the region of interaction is taken to be a sphere of absorbing material of uniform density with radius 0.93×10^{-13} cm. The absorption coefficient of nucleonic matter then varies from 4.3×10^{13} cm$^-$ at 0.81 Bev to 2.7×10^{13} cm^{-1} at 2.75 Bev. These parameters are purely empirical, and we have no theoretical justification for assuming an interaction region of this kind.

At 0.81 Bev only one pion appears to be produced, but at higher energies multiple pion production becomes increasingly frequent. At 2.75 Bev the percentages of inelastic events involving single, double, and triple pion production are estimated to be 36%, 48%, and 16%. Multiple pion production is thus considerably more common than predicted by the Fermi statistical theory, but not quite as common as the predictions of Kovacs, whose calculation takes into account a strong pion-nucleon final state interaction. Qualitatively, however, the Kovacs theory leads to predicted energies at which double and triple pion production should begin to become appreciable that are in rough agreement with experiment.

In single pion production events the $(pn+)$ reaction predominates at all energies. The $(pn+)/(pp0)$ ratio is 17 ± 8 at 0.81 Bev and remains high at the higher energies. An analysis in terms of charge independence shows that the predominant final state has a (real space) $\times$ (real spin) wave function, Φ_S, that is symmetric under exchange of the two nucleons, and corresponds to final state nucleons coupled with isotopic spin $T'=0$. Accordingly, proton and neutron should exhibit approximately identical spatial behavior. The momentum spectra, Q-value distributions, and angular distributions of the protons and neutrons are reasonably alike, which provides a rest of charge independence at energies considerably higher than those of previous tests. At 1.5 and 2.75 Bev charge-state ratios and spatial distributions are less well determined. The data involve no contradictions of charge independence.

Nucleons from inelastic collisions tend to be emitted forwards and backwards in the c.m. system so that relatively low momentum transfer is involved. Their angle and momentum distributions show marked devia-

tions from the predictions of the Fermi statistical theory at 1.5 Bev.

Correspondingly, pions tend to be emitted with low momenta, which is in marked disagreement with the predictions of statistical theory at 1.5 Bev. These data suggest that a π-nucleon interaction may affect pion production in an important way. Such a π-nucleon interaction might be strong in a $T=J=3/2$ resonant state, but our data are not sufficiently accurate to establish such details.

K. ACKNOWLEDGMENTS

APPENDIX. GENERAL RESULTS FROM CHARGE INDEPENDENCE CONCERNING $(pn+)$ AND $(pp0)$ REACTIONS

We wish to develop, from the charge-independence hypothesis, some general results for the reactions $p+p \rightarrow p+n+\pi^+$ and $p+p \rightarrow p+p+\pi^0$. The procedure resembles those applied for lower energies,[26] but here it is not possible to introduce the usual limitation to S and P states.

Since the initial p-p state of our system has isotopic spin $T=1$, $T_z=+1$, we require that our final system, consisting of two nucleons and a pion, be in a $(1, +1)$ state. Within the context of charge independence, the two nucleons in the final state must be treated as identical particles, since the charge state of a given nucleon is merely an additional quantum number specified by its z component of isotopic spin. This requires that the total final state wave function (depending on nucleons 1 and 2 and the pion), which is a product of (real space) $\times$ (real spin) $\times$ (isotopic spin) wave functions, be antisymmetric in the exchange of nucleons 1 and 2. (Hereafter, the terms symmetric and antisymmetric, and/or subscripts S and A will denote wave functions which are symmetric or antisymmetric under the exchange of two nucleons.)

The final-state isotopic spin wave function corresponding to an isotopic spin T can be constructed by first coupling the isotopic spin of the nucleons to obtain $T'=0$ or 1 and then combining T' with the isotopic spin of the meson to get T. This mode of intermediate coupling insures that the final isotopic spin state is either symmetric or antisymmetric. We find that the final isotopic spin wave functions corresponding to the two different intermediate values of T' are

$$\tau_A \equiv \frac{1}{\sqrt{2}}\left| p_1 n_2 + \right\rangle - \frac{1}{\sqrt{2}}\left| n_1 p_2 + \right\rangle \quad \text{for} \quad T'=0, \qquad (A.1)$$

$$\tau_S \equiv -\frac{1}{2}\left| p_1 n_2 + \right\rangle - \frac{1}{2}\left| n_1 p_2 + \right\rangle + \frac{1}{\sqrt{2}}\left| p_1 p_2 0 \right\rangle$$
$$\text{for} \quad T'=1, \qquad (A.2)$$

where, for example, $|p_1 n_2 +\rangle$ is the orthonormal state function for nucleon 1 being in a proton state (i.e., $t_{z1} = +1/2$), nucleon 2 being in a neutron state and the pion being in a π^+ state. We note that from (A.1) τ_A is antisymmetric, whereas from (A.2) τ_S is symmetric. If we denote the (real space)$\times$(real spin) portions of the outgoing wave function by Φ, then the total wave function Ψ (which is a function of the two nucleons and the pion) is

$$\Psi = \Phi_S \tau_A + \Phi_A \tau_S, \qquad (A.3)$$

where the appropriate (real space)$\times$(real spin) portion with τ_A must be symmetric in order to insure that Ψ be antisymmetric, and for the same reason, the (real space)$\times$(real spin) portion with τ_S must be antisymmetric. By combining (A.1), (A.2), and (A.3), the total wave function can be written as

$$\Psi = \left(-\frac{\Phi_A}{2} + \frac{\Phi_S}{\sqrt{2}} \right) \Big| p_1 n_2 + \Big\rangle$$
$$+ \left(-\frac{\Phi_A}{2} - \frac{\Phi_S}{\sqrt{2}} \right) \Big| n_1 p_2 + \Big\rangle + \frac{\Phi_A}{\sqrt{2}} \Big| p_1 p_2 0 \Big\rangle. \quad (A.4)$$

From (A.4) it can be shown that the ratio $r = d\sigma(pn+)/d\sigma(pp0)$ is given by

$$r = 1 + 2|\Phi_S|^2 / |\Phi_A|^2. \qquad (A.5)$$

Thus an experimental determination of r fixes the ratio $|\Phi_S|^2 / |\Phi_A|^2$. In particular, if $\Phi_S = 0$, then $r = 1$, whereas if $\Phi_A = 0$, $r = \infty$; i.e., $1 \leq r \leq \infty$.

If we consider the case $r = \infty$, (A.4) can be written as

$$\Psi = \frac{\Phi_S}{\sqrt{2}} \Big| p_1 n_2 + \Big\rangle - \frac{\Phi_S}{\sqrt{2}} \Big| n_1 p_2 + \Big\rangle. \qquad (A.6)$$

It follows from (A.6) that the real-space and real-spin distributions of the nucleons remain the same under the interchange of the charge states of nucleons 1 and 2, i.e., in the reaction $p + p \rightarrow p + n + \pi^+$, the spatial distributions for neutrons and protons must be *identical* for the final-state neutrons and protons. This conclusion remains unaltered for the case $r = 1$, as is seen from inspection of (A.4). Thus, in summary, if experiment were to show that r is given by either $r = \infty$ or $r = 1$, then it is predicted as a consequence of charge independence that the angular distributions, momentum distributions, etc., of the protons and neutrons in the aforementioned reaction would be identical.

These considerations permit us to construct a statistical theory which is a modification of that proposed by Fermi.[17] The Fermi statistical theory predicts no difference in spatial behavior between proton and neutron. We can use this property, conversely, to define what is meant by a statistical theory. If we do so, and require that the neutron and proton enter symmetri-

cally, it follows from Eq. (A.4) that

$$\left| -\frac{\Phi_A}{2} + \frac{\Phi_S}{\sqrt{2}} \right|^2 = \left| -\frac{\Phi_A}{2} - \frac{\Phi_S}{\sqrt{2}} \right|^2, \qquad (A.7)$$

if the neutron and proton are to have the same distributions for $(pn+)$ or $(pp0)$ reactions. Equation (A.7) can be satisfied in three ways: (a) $\Phi_A = 0$, (b) $\Phi_S = 0$, or (c) $\Phi_S = 0$ when $\Phi_A \neq 0$, and $\Phi_A = 0$ when $\Phi_S \neq 0$, but neither Φ_S nor Φ_A need be zero over all regions of space. Fermi apparently chose condition (c) and, to satisfy his statistical requirement took the average values of $|\Phi_A|^2$ and $|\Phi_S|^2$, integrated over all space, to be equal. This leads to an over-all ratio $R = 3$ for $\sigma_{tot}(pn+)/\sigma_{tot}(pp0)$. It would, however, be equally consistent with our definition of a statistical theory to choose either condition (a) or (b). The exclusion of the other symmetry state could then be due to a selection rule. In summary it is found that there are three *a priori* predictions of R possible from the statistical theory, corresponding to assumption (a), (b), and (c), respectively, $R = \infty$, $R = 1$, and $R = 3$. It should be observed that the large experimental values of R are in agreement with condition (a), and therefore, we conclude that these results are in essential agreement with the statistical theory, even though they disagree with the R value derived from the more restrictive conditions chosen by Fermi. These same remarks would apply to the modified statistical theory of Lepore and Neuman.[21]

One can also present an analogous formulation of the excited-state model. It is now assumed that nucleon 1 and the pion are coupled together in either a 3/2 or 1/2 isotopic spin state, which resultant is then coupled to nucleon 2 to lead to a final isotopic spin state for the 3 particles of $T = 1$, $T_z = +1$. These isotopic spin wave functions are labeled by the value of the intermediate state, and are given by

$$\tau_{\frac{3}{2}}(1,2) = -\frac{1}{\sqrt{6}} \Big| p_1 p_2 0 \Big\rangle$$
$$-\frac{1}{\sqrt{12}} \Big| n_1 p_2 + \Big\rangle + \frac{\sqrt{3}}{2} \Big| p_1 n_2 + \Big\rangle, \quad (A.8)$$

$$\tau_{\frac{1}{2}}(1,2) = -\frac{1}{\sqrt{3}} \Big| p_1 p_2 0 \Big\rangle + \frac{\sqrt{2}}{\sqrt{3}} \Big| n_1 p_2 + \Big\rangle. \qquad (A.9)$$

The indices 1,2 refer to the spatial positions of nucleons 1 and 2, and for simplicity, the pion position is omitted throughout. If nucleons were nonidentical particles, the total wave function would be given by

$$\Psi(1,2) = \Phi_{\frac{3}{2}}(1,2)\tau_{\frac{3}{2}}(1,2) + \Phi_{\frac{1}{2}}(1,2)\tau_{\frac{1}{2}}(1,2), \quad (A.10)$$

where the Φ's correspond to the (real space)$\times$(real spin) portion of the outgoing wave function. Since nucleons are identical particles (within the framework of charge

independence), and we thus require $\Psi(1,2) = -\Psi(2,1)$, Eq. (A.10) is clearly an inadmissible wave function in general. To give it the necessary antisymmetry, we form

$$\Psi(1,2) = \Phi_{\frac{3}{2}S}(1,2)\tau_{\frac{3}{2}A}(1,2) + \Phi_{\frac{3}{2}A}(1,2)\tau_{\frac{3}{2}S}(1,2)$$
$$+\Phi_{\frac{1}{2}S}(1,2)\tau_{\frac{1}{2}A}(1,2) + \Phi_{\frac{1}{2}A}(1,2)\tau_{\frac{1}{2}S}(1,2), \quad \text{(A.11)}$$

where

$$\tau_{\frac{3}{2}S}(1,2) = \frac{1}{\sqrt{2}}[\tau_{\frac{3}{2}}(1,2) + \tau_{\frac{3}{2}}(2,1)],$$

$$\tau_{\frac{3}{2}A}(1,2) = \frac{1}{\sqrt{2}}[\tau_{\frac{3}{2}}(1,2) - \tau_{\frac{3}{2}}(2,1)], \quad \text{(A.12)}$$

and

$$\Phi_{\frac{3}{2}S}(1,2) = \frac{1}{\sqrt{2}}[\Phi_{\frac{3}{2}}(1,2) + \Phi_{\frac{3}{2}}(2,1)],$$

$$\Phi_{\frac{3}{2}A}(1,2) = \frac{1}{\sqrt{2}}[\Phi_{\frac{3}{2}}(1,2) - \Phi_{\frac{3}{2}}(2,1)], \quad \text{(A.13)}$$

and similarly for the 1/2 state. These are functions of manifest symmetry and obviously lead to (A.11) being antisymmetric. We find from (A.12) and its analog for the 1/2 state that

$$\tau_{\frac{3}{2}S} = -(\tfrac{2}{3})^{\frac{1}{2}}\tau_S, \qquad \tau_{\frac{3}{2}A} = (4/3)^{\frac{1}{2}}\tau_A, \quad \text{(A.14)}$$

$$\tau_{\frac{1}{2}S} = -(4/3)^{\frac{1}{2}}\tau_S, \qquad \tau_{\frac{1}{2}A} = -(\tfrac{2}{3})^{\frac{1}{2}}\tau_A, \quad \text{(A.15)}$$

where τ_S and τ_A have been defined in (A.1) and (A.2).

Using (A.14), (A.15), and (A.11), the total wave function is found to be

$$\Psi = [(4/3)^{\frac{1}{2}}\Phi_{\frac{3}{2}S} - (\tfrac{2}{3})^{\frac{1}{2}}\Phi_{\frac{1}{2}S}]\tau_A$$
$$+[-(\tfrac{2}{3})^{\frac{1}{2}}\Phi_{\frac{3}{2}A} - (4/3)^{\frac{1}{2}}\Phi_{\frac{1}{2}A}]\tau_S. \quad \text{(A.16)}$$

Comparison of (A.16) with (A.3) indicates that the wave function Φ_A and Φ_S previously obtained can be interpreted, in the excited nucleon model, as being given by

$$\Phi_S = (4/3)^{\frac{1}{2}}\Phi_{\frac{3}{2}S} - (\tfrac{2}{3})^{\frac{1}{2}}\Phi_{\frac{1}{2}S}, \quad \text{(A.17)}$$

and

$$\Phi_A = -(\tfrac{2}{3})^{\frac{1}{2}}\Phi_{\frac{3}{2}A} - (4/3)^{\frac{1}{2}}\Phi_{\frac{1}{2}A}. \quad \text{(A.18)}$$

Under Peaslee's restrictive assumption that only the 3/2 isobar is formed, $\Phi_{\frac{1}{2}S} = \Phi_{\frac{1}{2}A} = 0$. Further, it is implicit and necessary in his calculation that the isobar be assumed to have a sufficiently long lifetime so that on the average it decays when it is quite separated from the other nucleon, and thus is not interacting with it. Under these conditions, the spatial portion of the wave function containing the two nucleons can be separated into forms of the type $(1/\sqrt{2})[f(1)g(2) \pm f(2)g(1)]$. If nucleon 1 (the one assumed to be coupled to the pion in the case of nonidentical nucleons) is sufficiently localized so that it has an appreciable wave function only in the neighborhood of position 1, then $\Phi_{\frac{3}{2}S}(1,2) \approx \Phi_{\frac{3}{2}A}(1,2) \approx (\tfrac{1}{2})^{\frac{1}{2}}\Phi_{\frac{3}{2}}(1,2)$, where $\Phi_{\frac{3}{2}}(1,2)$ is the unsymmetrized wave function in (A.10). In this limit,

$$\Phi_S \approx (\tfrac{2}{3})^{\frac{1}{2}}\Phi_{\frac{3}{2}}, \quad \text{and} \quad \Phi_A \approx -(\tfrac{1}{3})^{\frac{1}{2}}\Phi_{\frac{3}{2}}. \quad \text{(A.19)}$$

Therefore, from (A.5), we obtain $r=5$ at all angles and momenta, so that the over-all ratio R is also 5, the result obtained by Peaslee. If we were to have made the opposite assumption, that only the 1/2 state isobar contributes to the process, the corresponding value of R would be 2. Values of R larger than 5 and smaller than 2 can only occur because of interference terms between the 3/2 and 1/2 states.